Manganese(II) Alkyl / π-Allyl Complexes Resistant to Ligand Redistribution

Preeti Chadha,[a] *David J. H. Emslie*[a,]* *and Hilary A. Jenkins*[b]

[a] Department of Chemistry and Chemical Biology, McMaster University, Hamilton, Ontario, L8S 4M1, Canada. Fax: (01) 905 522 2509; Tel: (01) 905 525 9140 x 23307; E mail: emslied@mcmaster.ca

[b] McMaster Analytical X-Ray Diffraction Facility, Department of Chemistry and Chemical Biology, McMaster University, Hamilton, Ontario, L8S 4M1, Canada.

ABSTRACT

Reaction of $[Li(THF)_4][(Mn\{C(SiMe_3)_3\})_3(\mu\text{-}Cl)_4(THF)]$ (**1**) with $K(allyl^{TMS2})$ $\{allyl^{TMS2} = 1,3\text{-}C_3H_3(SiMe_3)_2\}$ afforded $[(\eta^3\text{-}allyl^{TMS2})Mn\{C(SiMe_3)_3\}\{ClLi(THF)_3\}]$ (**2**). Attempted sublimation of **2** yielded $[(\eta^3\text{-}allyl^{TMS2})Mn\{C(SiMe_3)_3\}(THF)]$ (**3**), indicating that **2** extrudes LiCl at elevated temperatures. Additionally, LiCl in **2** was displaced by reaction with PMe_3, quinuclidine and dmap {dmap = 4-(dimethylamino)pyridine}, providing $[(\eta^3\text{-}allyl^{TMS2})\text{-}Mn\{C(SiMe_3)_3\}(L)]$ (L = PMe_3 (**4**), quinuclidine (**5**), and dmap (**6**)]. Treatment of PMe_3 complex **4** with BPh_3 yielded bright red $[(allyl^{TMS2})Mn\{C(SiMe_3)_3\}]$ (**7**) accompanied by a precipitate of $Ph_3B(PMe_3)$. Mixed alkyl / π-allyl manganese(II) complexes **2**-**7** are pyrophoric red solids with a high-spin d^5 configuration, and all were crystallographically characterized. In the solid state structures, the allyl ligands in **2**-**6** adopt a *syn*,*syn*-configuration, whereas in base-free **7**, the allyl ligand has a *syn*,*anti*-configuration. Complexes **4**, **5** and **7** sublimed cleanly (5 mTorr) at 70, 90 and 50 °C, respectively. Complex **4** exhibited a particularly favourable combination of volatility and thermal stability given that its appearance and powder X-ray diffraction pattern were unchanged after 24 hours in a sealed flask at 100 °C. Compounds **2**-**7** are the first high-spin d^5 mixed alkyl / allyl complexes, and **7** is the first room-temperature-stable example of a mononuclear transition metal complex bearing only alkyl and allyl ligands.

Introduction

Base-free and oligomeric $[Mn(CH_2CMe_2Ph)_2]_2$, $[Mn(CH_2CMe_3)_2]_4$ and $[Mn(CH_2SiMe_3)_2]_x$ were reported by Wilkinson in 1976,[1] and various Lewis base adducts of these compounds (with monometallic or dimetallic structures) were subsequently described.[2,3] The range of well-characterized manganese(II) dialkyl complexes was also expanded through the use of alternative alkyl groups including CH_3, CH_2Ph, Cy, $CH(SiMe_3)_2$, CMe_3 and $C(SiMe_3)_3$.[2,4,5] By comparison, neutral manganese(II) diallyl complexes are limited to $[(\eta^1\text{-allyl}^{TMS2})_2Mn(THF)_2]$ and $[(\eta^1\text{-allyl}^{TMS3})_2Mn(tmeda)]$ $\{\text{allyl}^{TMS2} = 1,3\text{-}C_3H_3(SiMe_3)_2;\ \text{allyl}^{TMS3} = 1,2,3\text{-}C_3H_2(SiMe_3)_3\}$,[6] and mixed alkyl / allyl manganese(II) complexes are unknown. In fact, although alkyl and allyl ligands play a central role in organometallic chemistry, complexes containing both alkyl and allyl ligands are uncommon throughout the transition series[7-17] (see Figure 1 for examples of open-shell mixed alkyl / allyl complexes and transition metal compounds bearing only alkyl and allyl ligands), likely in large part due to the propensity of mixed hydrocarbyl complexes to engage in ligand redistribution reactions. Such reactions have been noted to be particularly facile for manganese(II) complexes with a high-spin d^5 configuration as a result of the weak and polar bonds that result from an absence of ligand field stabilization energy. These same factors have also been cited to explain why many high-spin organomanganese(II) complexes have more in common with main group analogues than transition metal complexes,[6,18,19] to the extent that manganese(II) has been branded the "black sheep of the organometallic family".[20]

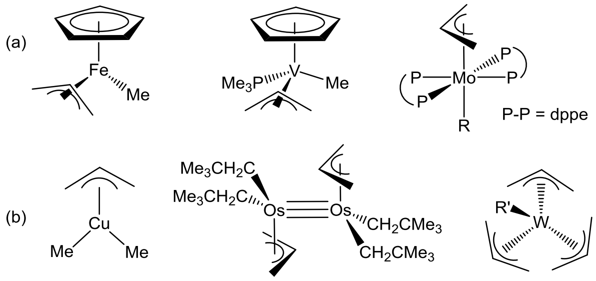

Figure 1. (a) Open-shell alkyl / allyl complexes (R = Me, CH_2SiMe_3). (b) Transition metal compounds bearing *only* alkyl and allyl ligands (R' = Me, Et, ^{n}Pr, ^{i}Pr, ^{n}Bu, ^{n}Pent). Analogues of the copper(III) complex with substituents at various positions on the allyl ligand are also known.

In the broad context of developing new precursors for CVD and ALD of manganese-containing films,[21] we were interested to explore the stability and volatility of bis-hydrocarbyl manganese(II) complexes in which α-hydrogen abstraction and β-hydrogen elimination are prevented or disfavored. Monomeric $[Mn\{C(SiMe_3)_3\}_2]$[5] was particularly attractive in this regard, but in our hands the reported synthesis afforded mostly $[Li(THF)_4][(Mn\{C(SiMe_3)_3\})_3(\mu\text{-}Cl)_4(THF)]$ (**1**)[22] with less than a ten percent yield of $[Mn\{C(SiMe_3)_3\}_2]$, even when the reaction time was extended to 1 week. Given that allyl ligands are typically resistant to hydrogen abstraction/elimination reactions, we turned our attention to the synthesis of mixed $C(SiMe_3)_3$ / allyl^{TMS2} complexes using **1** as the starting material. We reasoned that a single extremely bulky $C(SiMe_3)_3$ ligand may be sufficient to impart a high level of thermal stability, and that the decreased steric bulk of the target complexes relative to $[Mn\{C(SiMe_3)_3\}_2]$ may allow their synthesis in high yield. Hetero-hydrocarbyl complexes of this type are also of interest due to their potential to exhibit unique volatility and reactivity characteristics relative to homo-hydrocarbyl complexes, especially when the hydrocarbyl ligands are sterically and/or electronically dissimilar. Herein we describe the synthesis of the first high-spin d^5 mixed alkyl / π-allyl complexes; those of manganese(II).

Results and Discussion

Reaction of $[Li(THF)_4][(Mn\{C(SiMe_3)_3\})_3(\mu\text{-}Cl)_4(THF)]$ (**1**)[22] with K(allyl^{TMS2})[23,24] {allyl^{TMS2} = 1,3-$C_3H_3(SiMe_3)_2$} produced crude $[(\eta^3\text{-allyl}^{TMS2})Mn\{C(SiMe_3)_3\}\{ClLi(THF)_3\}]$ (**2**) as a deep red paramagnetic oil in 65% yield (Scheme 1), and crystallization from hexanes at –30 °C afforded bright red crystals of **2**. Attempted sublimation of **2** at 65 °C and 5 mTorr deposited a bright red oil on the cold finger, and crystallization from pentane at –30 °C provided red crystals of [(η^3-allyl^{TMS2})Mn{C(SiMe$_3$)$_3$}(THF)] (**3**; *vide infra*), indicating that **2** extrudes LiCl at elevated temperatures. Additionally, LiCl in **2** was displaced by reaction with PMe$_3$, quinuclidine and dmap {dmap = 4-(dimethylamino)-pyridine} yielding [(η^3-allyl^{TMS2})Mn{C(SiMe$_3$)$_3$}(L)] (L = PMe$_3$ (**4**), quinuclidine (**5**), and dmap (**6**)] (Scheme 1). Complexes **4-6** were isolated in good yields as pyrophoric red powders, and are the first neutral π-allyl complexes of manganese(II). Previously reported open-shell mixed alkyl / allyl complexes are limited to [CpFeMe(η^3-allyl)],[12] [CpVMe(η^3-allyl)(PMe$_3$)] and [MoR(η^3-allyl)(dppe)$_2$] (R = Me or CH$_2$SiMe$_3$)[16] (Figure 1), and none of these compounds have been structurally characterized.

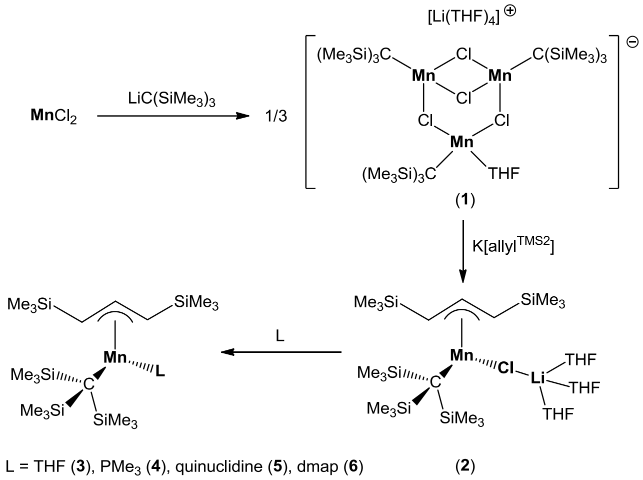

Scheme 1. Synthesis of mixed alkyl / allyl manganese complexes **2-6**.

Compounds **2-6** were characterized by X-ray crystallography (the structure of **2** is only suitable to establish connectivity),[25] and bulk sample purity was confirmed by powder X-ray diffraction and elemental analysis. Room temperature Evans magnetic measurements[26] on **2-6** yielded magnetic moments between 5.63 and 6.13 B.M. (± 0.3 B.M.), consistent with high-spin manganese(II), and ^{1}H NMR spectra consisted of two or three very broad peaks between 4 and 50 ppm. The X-ray crystal structures for **3**-**6** are shown in Figure 2 (see Figure S1 for the structure of **2**, and Table 1 for selected bond lengths and angles in **3**-**6**). In all cases the allyl ligand has a *syn*,*syn*-arrangement of the trimethylsilyl substituents, with the central C–H bond oriented towards the neutral donor, rather than the $C(SiMe_3)_3$ ligand. The Mn–C(1) and Mn–C(3) bond lengths are very similar in compounds **4**-**6** [for each compound, $\Delta(Mn–C^{1/3}) \leq 0.05$ Å], consistent with η^3-coordination. In comparison, Mn–C(1) is shorter in **3** than in **4**-**6**, and Mn–C(3) is longer [$\Delta(Mn–C^{1/3}) = 0.23$ Å], indicative of some distortion in the direction of η^2-coordination.

The centroid of the allyl ligand, Mn, C(4) and E (E = Cl, O, P or N) lie approximately in a plane, and the C(1)–Mn–C(3) plane lies perpendicular to the C(4)–Mn–E plane. Complexes **2**-**6** are therefore tetrahedral 13-electron analogues of known square planar [(η^3-allyl)M(alkyl)(L)] (M = Ni and Pd).[10] The Mn–C(4) distances in **3**-**6** range from 2.14 to 2.19 Å, while the Mn–C_{allyl} distances are longer at 2.31-2.40 Å for **4**-**6** and 2.27-2.50 Å for **3**. The Mn–E distances are 2.170(3) Å (E = O in **3**), 2.617(1) Å (E = P in **4**), 2.258(4) and 2.270(4) Å (E = N_{sp3} in **5**), and 2.163(4) Å (E = N_{sp2} in **6**). The shorter Mn–N distance in **6** vs **5** indicates more effective binding of dmap than quinuclidine, and the increasing Mn–E_{sp3} distances in the order **3** < **5** < **4** mirror the trend in the covalent radii.[27] The C(4)–Mn–E (E = O, P and N) angles in **3** and **6** are 119-122°, compared with 126° and 129-131° in **4** and **5**, respectively. This increase is presumably steric in origin, and is accompanied by a decrease in the allyl$_{centroid}$–Mn–C(4) angle; from 135-137° in **3** and **6** to 131° in **4** and 125-127° in **5**.

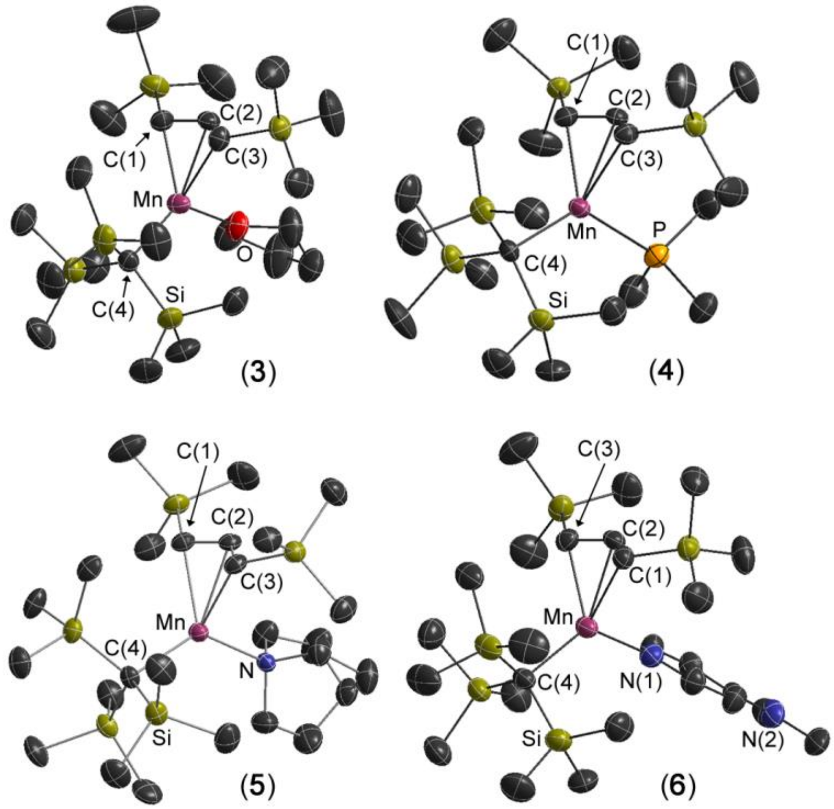

Figure 2. X-ray Crystal Structures of [(η^3-allyl^{TMS2})Mn{C(SiMe$_3$)$_3$}(L)] [L = THF (**3**), PMe$_3$ (**4**), quinuclidine (**5**), and dmap (**6**)]. Hydrogen atoms are omitted for clarity and ellipsoids are at 50 %.[25,28]

Compound	**3**	**4**	**5**	**6**	**7**
Mn–C(1)	2.268(4)	2.342(3)	2.355(4), 2.355(4)	2.343(5)	2.174(1)
Mn–C(2)	2.321(4)	2.327(3)	2.356(4), 2.358(4)	2.312(4)	2.300(1)
Mn–C(3)	2.496(4)	2.349(3)	2.365(5), 2.390(4)	2.397(5)	2.510(1)
Mn–C(4)	2.144(4)	2.164(3)	2.187(4), 2.181(5)	2.167(5)	2.092(1)
Mn–E	2.170(3)	2.617(1)	2.270(4), 2.258(4)	2.163(4)	---
C(1)–C(2)	1.420(5)	1.403(4)	1.403(6), 1.409(6)	1.412(6)	1.435(2)
C(3)–C(4)	1.384(5)	1.404(4)	1.410(6), 1.413(6)	1.395(6)	1.383(2)
C(4)–Mn–E	118.7(1)	125.90(7)	130.5(2), 128.9(2)	122.4(2)	---
Cent–Mn–E	103.2	103.4	104.8, 104.5	102.7	---
Cent–Mn–C(4)	137.4	130.7	124.7, 126.6	134.8	166.3

Table 1. Bond lengths (Å) and angles (°) for compounds **3**-**7**. Only one of the two independent molecules of **3** in the unit cell is free from disorder; bond lengths and angles are provided for this molecule.[25,28]

Complexes **4** and **5** sublimed (5 mTorr) cleanly at 70 and 90 °C, respectively. By contrast, **6** sublimed at 115 °C (5 mTorr) with accompanying decomposition, and pure samples were only obtained by crystallization. Complex **4** exhibited a particularly favourable combination of volatility and thermal stability given that its appearance and powder X-ray diffraction pattern were unchanged after 24 hours in a sealed flask under argon at 100 °C. However, in a flask open to argon, decomposition was evident after 12 hours at 100 °C, suggesting that reversible PMe_3 dissociation (to form **7** in situ; *vide infra*) precedes thermal decomposition. In accord with this hypothesis, simultaneous TGA/DSC (10 °C / min) at 760 Torr revealed a clean mass loss step of 14 wt% from 50 to 130 °C, consistent with PMe_3 dissociation (calcd. 14 wt%). A subsequent mass loss step suggests volatilization of the PMe_3-free complex, but it is accompanied by thermal decomposition just below 200 ^oC. By contrast, TGA performed at 0.5 Torr (10 °C / min) led to much more rapid mass loss between 80 and 125 ^oC, with competing PMe_3 loss and bulk sample volatilization suggested by DSC analysis. At 225 °C, the residual mass was 2%, indicative of volatilization of the majority of the sample.[29]

The high thermal stability of compounds **2**-**6** is remarkable given (a) their high-spin d^5 configuration, which typically results in a susceptibility towards ligand redistribution,[2,14] and (b) the steric accessibility of the products of ligand redistribution (homoleptic bis-hydrocarbyl manganese complexes), as evidenced by $[Mn\{C(SiMe_3)_3\}_2]$,[5] $[Li(THF)_4][Mn\text{-}(allyl^{TMS2})_3]$,[30] and $K_2[Mn(allyl^{TMS2})_4]$.[6] Several features are likely responsible for the high thermal stability of **2**-**6**: a favourable level of steric hindrance, the absence of α- and β-hydrogen atoms in the alkyl ligand, and the η^3-coordination mode of the allyl ligand which may help to prevent ligand transfer via μ-allyl intermediates.

Treatment of PMe_3 complex **4** (^1H NMR δ 12 and 41 ppm) with BPh_3 yielded bright red $[(allyl^{TMS2})Mn\{C(SiMe_3)_3\}]$ (**7**; *vide infra*) accompanied by a precipitate of $Ph_3B(PMe_3)$ (Scheme 2). Pure **7** was obtained by filtration in pentane followed by sublimation at 50 °C (5 mTorr), and showed no sign of decomposition after 1 week in C_6D_6 at room temperature.[31] Complex **7** has five unpaired electrons by Evans magnetic measurement, displays a distinctive ^{1}H NMR spectrum with broad signals at 22 and 69 ppm, and reacted cleanly with PMe_3 and dmap to form **4** and **6**, respectively. Samples of **7** solidified after days to weeks at –25 °C, and melted at 41 °C (determined by DSC). The low melting point and sublimation temperature of **7** are suggestive of a monomeric reaction product or a product that readily dissociates to monomeric units.

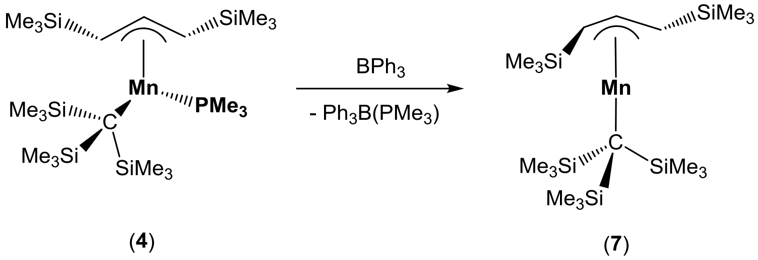

Scheme 2. Synthesis of base-free **7** by PMe_3 abstraction from **4**. Compound **7** is depicted with a *syn*,*anti*-configuration of the allyl ligand in order to match the X-ray crystal structure. However, we cannot exclude the possibility that the bulk sample contains a mixture of the *syn*,*syn*- and *syn*,*anti*-isomers.

X-ray quality crystals of **7** were obtained from a highly concentrated pentane solution at –25 °C, confirming a monomeric structure (Figure 3; Table 1). Unexpectedly, the trimethylsilyl groups of the allyl^{TMS2} ligand now adopt a *syn*,*anti*- rather than a *syn*,*syn*-arrangement, implying isomerization *via* an η^1-allyl structure. We were not able to determine conclusively whether the bulk sample of **7** consists only of the *syn*,*anti*-isomer or a mixture of the *syn*,*anti*- and *syn*,*syn*-isomers due to the paramagnetism and low melting point of **7**, which prevented packing and sealing of a sample in a capillary for PXRD. However, observation of a single melting point at 41 °C in the DSC of **7** is strongly suggestive of a single isomer; presumably the *syn*,*anti*-isomer. The $C(SiMe_3)_3$ anion in the structure of **7** is positioned approximately trans to the allyl^{TMS2} ligand, with a C(4)–Mn–allyl$_{centroid}$ angle of 166°. Compared with **2-6**, the Mn–C(4) distance in **7** is shorter [2.092(1) vs 2.164(3) Å], and the allyl bonding mode is significantly less symmetrical, tending in the direction of η^2-coordination [Mn–C(1) = 2.174(1) Å, Mn–C(2) = 2.300(1) Å, Mn–C(3) = 2.510(1) Å; C(1)–C(2) = 1.435(2) Å; C(2)–C(3)= 1.383(2) Å].

Complexes containing *only* alky and allyl ligands are limited to 16-electron [(η^3-allyl)Cu^{III}R$_2$],[32] [(η^3-allyl)$_3$W^{IV}(alkyl)] (R = Me, Et, ^{n}Pr, ^{i}Pr, ^{n}Bu and ^{n}Pent),[33] and [{Os^{III}(CH$_2$CMe$_3$)$_2$(η^3-allyl)}$_2$][34] (Figure 1). Only the latter complex, which features an Os≡Os triple bond, is stable at room temperature; the copper(III) complexes were detected by direct injection NMR spectroscopy at –100 °C, and the tungsten(IV) complexes decomposed between –78 and 0 °C, depending on the nature of the R group. Compound **7** is therefore the only room temperature-stable example of a monometallic transition metal complex that is ligated solely by alkyl and allyl ligands.

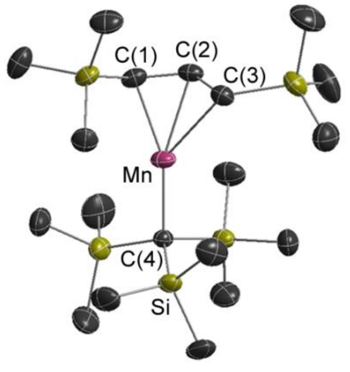

(**7**)

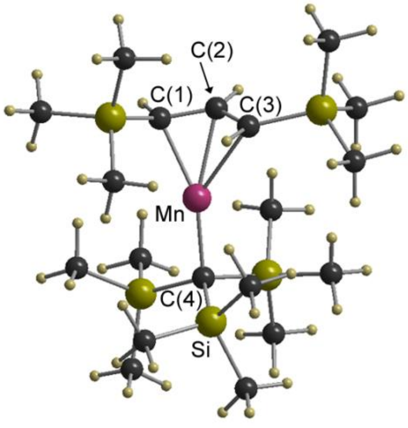

Calculated **7**

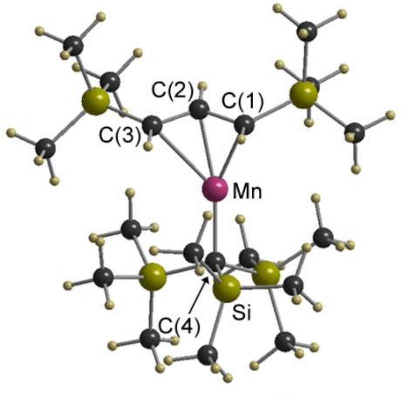

Calculated **7**^{ss}

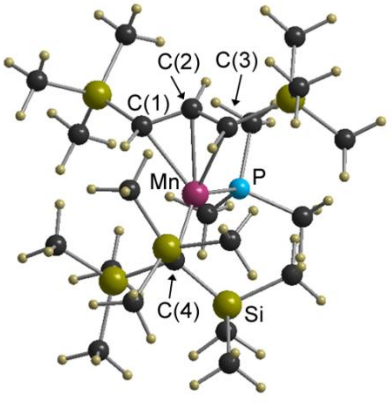

Calculated **4**

Figure 3. Top Left: X-Ray Crystal Structure of [(*syn*,*anti*-allyl^{TMS2})Mn{C(SiMe$_3$)$_3$}] (**7**). Hydrogen atoms are omitted and ellipsoids are at 50 %. Top right: Calculated structure of **7**. Bottom left: Calculated structure of **7**^{ss}; [(*syn*,*syn*-allyl^{TMS2})Mn{C(SiMe$_3$)$_3$}]. Bottom right: Calculated structure of PMe$_3$ complex **4**.

DFT calculations were carried out on **4** and **7** (ADF 2013.1, PBE, D3-BJ, TZ2P all-electron, unrestricted, 5 unpaired electrons, ZORA), and the geometries show reasonable agreement with the X-ray crystal structures (Tables S1). Consistent with the slippage towards a more η^2-coordinated structure in **7**, the sum of the calculated C–C–Si, C–C–H and Si–C–H angles around C(1) and C(3) in **7** are 351 and 358°, respectively, compared with 355° around both C(1) and C(3) in compound **4**. Calculations on [(allyl^{TMS2})Mn{C(SiMe$_3$)$_3$}] with a *syn*,*syn*-arrangement of the trimethylsilyl groups yielded a structure (**7**^{ss}; Figure 3) with a similarly asymmetric allyl bonding mode to that of **7**, but a Gibbs free energy that is 13 kJ mol^{-1} higher at 298 K, corresponding to an equilibrium constant approaching 200 in favour of **7**. The favourability of a strongly asymmetric allyl bonding mode in **7** [calculated Δ(Mn–C$^{1/3}$) = 0.33 Å] may derive in part from close approach between the SiMe$_3$ groups of the allyl and alkyl ligands, given that the structures for hypothetical [(*syn*,*anti*-allyl^{TMS2})MnR] {R = C(SiH$_3$)$_3$ and Me} feature an allyl ligand that is more symmetrically coordinated {Δ(Mn–C$^{1/3}$) = 0.10-0.12 Å}.[35] In addition, hypothetical [(*syn*,*syn*-allyl^{TMS2})MnH] and [(allyl)MnH] were previously calculated to be C_s symmetric.[6] However, restraining the Mn-C(1) and Mn-C(3) bonds in **7** to be equal and allowing them to refine freely as a single variable led to an η^3-allyl structure {**7'**; Mn–C(1) = Mn–C(3) = 2.30 Å} that is only 2 kJ mol^{-1} higher in Gibbs free energy at 298 K. The very small ΔG between **7** and **7'** suggests that **7** will be fluxional, with facile access to η^2 and η^3 allyl bonding modes. By contrast, enforcing an

η^1-allyl coordination mode[36] yielded a structure (**7''**) that is 25 kJ mol^{-1} higher in Gibbs free energy than **7** at 298 K.

Summary and Conclusions

The first alkyl / allyl complexes with a high-spin d^5 configuration have been synthesized; 13-electron [(allyl^{TMS2})Mn{C(SiMe$_3$)$_3$}(L)] {L = ClLi(THF)$_3$ (**2**), THF (**3**), PMe$_3$ (**4**), quinuclidine (**5**), dmap (**6**)} and 11-electron [(allyl^{TMS2})Mn(TSI)] (**7**). Compound **7** is a rare example of a mononuclear transition metal complex bearing only alkyl and allyl ligands, and is the only room-temperature-stable example. Given that high-spin d^5 complexes are noted for their susceptibility to ligand redistribution,[6,18] and homo-hydrocarbyl manganese(II) complexes bearing C{SiMe$_3$)$_3$ and allyl^{TMS2} ligands are known, [5,6,30] the thermal stability of **2-7** is remarkable. In fact, it suggests that bulky acyclic hydrocarbyl ligands may be suitable to stabilize a broad range of hetero-hydrocarbyl complexes that are free from multidentate or anionic supporting ligands. Complexes of this type have rarely been reported[37] but may be attractive as precursors with unique stability, volatility and reactivity profiles for organometallic synthesis, chemical vapor deposition (CVD) and atomic layer deposition (ALD).

Experimental Section

General Details. An argon-filled MBraun UNIlab glovebox was employed for the manipulation and storage of all oxygen and moisture sensitive compounds, and air-sensitive preparative reactions were performed on a double manifold high vacuum line using standard techniques. Compounds **2-7** are exceptionally air-sensitive, and most are pyrophoric. Residual oxygen and moisture was removed from the argon stream by passage through an Oxisorb-W scrubber from Matheson Gas Products. A VWR Clinical 200 Large Capacity Centrifuge (with 28° fixed-angle rotors that hold 12 × 15 mL or 6 × 50 mL tubes) in combination with VWR high-performance polypropylene conical centrifuge tubes was used when required (inside the glovebox). Vacuum was measured using a Varian model 531 Thermocouple Gauge Tube with a Model 801 Controller.

Anhydrous diethylether was purchased from Aldrich and then dried over sodium benzophenone ketyl. Hexanes, pentanes, THF were dried and distilled at atmospheric pressure from sodium benzophenone ketyl and toluene from sodium. Unless otherwise noted, all anhy- drous solvents were stored over an appropriate drying agent prior to use (OEt$_2$, THF, THF-d^8, toluene, d^8-toluene, C_6D_6 = Na/Ph$_2$CO; pentane, hexanes = Na/Ph$_2$CO/tetraglyme). Anhydrous MnCl$_2$, CoCp$_2$, BPh$_3$, KO^{t}Bu, CHBr$_3$, SiMe$_3$Cl, MeLi (1.6 M in Et$_2$O), ^{n}BuLi (1.6 M in hexane), ^{s}BuLi (1.4 M in cyclohexane), 3-(Trimethylsilyl)propene (abbreviated as H[allyl^{TMS}]), PMe$_3$, quinuclidine and 4-dimethylaminopyridine (dmap) were purchased from Aldrich or Strem Chemicals. K[B(C$_6$F$_5$)$_4$] was purchased from Boulder Scientific. [NBu$_4$][B(C$_6$F$_5$)$_4$] was prepared via a slight modification of the original literature procedure[38] (using K[B(C$_6$F$_5$)$_4$] in place of Li(OEt$_2$)$_x$[B(C$_6$F$_5$)$_4$]) and dried thoroughly before use.

Diethylether was removed from a commercial MeLi solution and the resulting powder was stored in the glovebox. CHBr$_3$ was extracted 3-4 times with water, dried over CaCl$_2$, followed by activated molecular sieves, and then distilled prior to use.[39] H[allyl^{TMS}] and SiMe$_3$Cl were dried over CaH$_2$ and distilled before use. Quinuclidine and dmap were sublimed and BPh$_3$ was recrystallized from diethylether and dried *in vacuo* before use. HC(SiMe$_3$)$_3$,[40] LiC(SiMe$_3$)$_3$.2THF,[41] and Mn[C(SiMe$_3$)$_3$]$_2$ (in low yield)[5] were prepared as previously reported. H[allyl^{TMS2}],[42] and K[allyl^{TMS2}][23] were prepared following modifications of the literature procedures (see supporting information).

NMR spectroscopy (^{1}H, ^{11}B, ^{31}P{1H}) was performed on a Bruker DRX-500 spectrometer. All ^{1}H NMR spectra were referenced relative to SiMe$_4$ through a resonance of the employed deuterated solvent or proteo impurity of the solvent; C_6D_6 (δ 7.16 ppm) and THF-d^8 (3.58, 1.73 ppm) for ^{1}H NMR. ^{11}B and ^{31}P NMR spectra were referenced using an external standard of BF$_3$(OEt$_2$) (0.0 ppm) and 85% H$_3$PO$_4$ in D$_2$O (0.0 ppm), respectively.

Combustion elemental analyses were performed on a Thermo EA1112 CHNS/O analyzer. Samples for elemental analysis (typically 2-4 mg) were packed and sealed in pre-weighed 3 x 6 mm smooth wall tin capsules inside the glovebox. After removal from the glove box, these capsules were packed into 5 x 8 mm pressed aluminium capsules containing approximately 10 mg of V$_2$O$_5$. DSC of **7** was performed on a TA instruments DSC 2910 using a 2.8 mg sample that was sealed into a hermetic aluminium pan inside the glove box. Simultaneous TGA/DSC was performed on a dual TA Instruments Q600 SDT within an argon-filled glove box at a typical rate of 10 ºC/min. Due to the high air and moisture sensitivity of the samples, crucibles (aluminum) were dried at 130 ºC under vacuum prior to use. Atmospheric pressure temperature ramps were performed using 100 mL/min flow rate of inert gas while reduced pressure measurements were performed under dynamic vacuum (0.5 Torr). Cyclic voltammetry (CV) studies were carried out using a PAR (Princeton Applied Research) model 283 potentiostat (using PAR PowerCV software) in conjunction with a three-electrode cell under an argon atmosphere. The auxiliary electrode was a platinum wire, the pseudo-reference electrode a silver wire, and the working electrode a glassy carbon disc (3.0 mm diameter, Bioanalytical Systems). Solutions were 1 x 10^{-3} M in test compound and 0.1 M in $[NBu_4][B(C_6F_5)_4]$ as the supporting electrolyte in dry THF. In all experiments, potentials were calibrated by addition of $[CoCp_2]$; the $E_{1/2}$ value for $[CoCp_2]^{0/+1}$ in THF / $[NBu_4][B(C_6F_5)_4]$ was measured to be −1.33 V vs $[FeCp_2]^{0/+}$.

Single-crystal X-ray crystallographic analyses were performed on crystals coated in Paratone oil and mounted on a SMART APEX II diffractometer with a 3 kW sealed tube Mo generator and SMART6000 CCD detector. Powder X-ray Diffraction (PXRD) experiments were performed on a Bruker D8 Advance Powder diffractometer with Cu Kα radiation (λ=0.154nm) operated at 40kV and 40mA. Powders were packed in 0.5 mm O.D. special glass (SG; wall thickness 0.01 mm) capillary tubes for X-ray diffraction (purchased from Charles Supper Company) and sealed by inverting to submerge the open end in a pool of Apiezon H-grease within a glove box. Calculated powder patterns for **2-7** were generated from the low-temperature single-crystal data and then refined using Topas 4.2 (Bruker software).

$[(allyl^{TMS2})Mn\{C(SiMe_3)_3\}\{ClLi(THF)_3\}]$ (2): Anhydrous $MnCl_2$ (2.38 g, 18.9 mmol) was ground to a fine powder and introduced in a round bottom flask. $LiC(SiMe_3)_3.2THF$ (7.23 g, 18.9 mmol) was weighed out in another flask. Both flasks were appended to a vacuum line and ~100 mL of THF was vacuum transferred to each flask. The $LiC(SiMe_3)_3.2THF$ solution was then added to the suspension of

$MnCl_2$ in THF at –78 °C *via* cannula. The cold bath was removed after an hour and the reaction mixture was allowed to stir at room temperature overnight (20 h) during which time the solution turned clear yellow. The reaction mixture, now containing $[Li(THF)_4][Mn_3\{C(SiMe_3)_3\}_3(\mu\text{-}Cl)_4]$, was cooled to –45 °C and a solution of K[allyl^{TMS2}] (4.24 g, 18.9 mmol; THF, 100 mL) was added dropwise *via* cannula. The reaction mixture turned red during addition. The cold bath was removed after 1 h and the reaction mixture was stirred at room temperature for 24 h. THF was then removed *in vacuo* and 100 mL of hexanes was introduced. After stirring for 1 h, hexane was also removed and the oily residue was taken in the glovebox. The residue was redissolved in 2:1 hexane:benzene mixture, centrifuged to remove white solids, the supernatant was collected and all solvents removed to obtain a dark red oil (9.0 g, 65%). Some of the oil was redissolved in hexanes to give a clear red solution, which yielded X-ray quality crystals over several days at –30 °C (if a small amount of oil initially precipitated, the mother liquors were decanted and returned to –30 °C for crystallization). The oil was used in all subsequent reactions. Crystalline samples were used for all spectroscopic and analytical measurements. ^{1}H NMR: (C_6D_6; δ) 4.5, 11.9, 34.1 ppm. ^{1}H NMR: (C_4D_8O; δ) 11.0, 29.2 ppm. EA (found/calculated): C (50.91/50.96), H (10.15/9.93) %. μ_{eff} = 6.08 B.M. E_{pa} = –0.16 V vs $[FeCp_2]^{0/+}$ in THF (ν = 200 mVs^{-1}).

[(allyl^{TMS2})Mn{C(SiMe$_3$)$_3$}(THF)] (3): Attempted sublimation of **2** (0.080 g, 0.11 mmol) at 65 °C yielded a red oil which was washed off the cold finger with the minimum volume of pentane and cooled to –30 °C, yielding X-ray quality crystals (0.050 g, 84%) over several days. ^{1}H NMR: (C_6D_6; δ) 14.4, 46.0 ppm. ^{1}H NMR: (C_4D_8O; δ) 10.9, 34.5 ppm. EA (found/calculated): C (50.81/50.78), H (10.62/10.37) %. μ_{eff} = 6.13 B.M. E_{pa} = –0.06 V vs $[FeCp_2]^{0/+}$ in THF (ν = 200 mVs^{-1}).

[(allyl^{TMS2})Mn{C(SiMe$_3$)$_3$}(PMe$_3$)] (4): Compound **2** (2.76 g, 3.78 mmol) was dissolved in hexanes (40 mL), PMe_3 (0.5 mL, 4.83 mmol) was introduced at room temperature, and the reaction was stirred overnight. No colour change was observed, but some white solids precipitated. The solution was evacuated to dryness *in vacuo* to remove any excess PMe_3 and then taken into the glovebox. The residue was redissolved in hexanes, centrifuged to remove solids, and the red solution was evaporated to dryness. The resulting red solid was sublimed at 70 °C (5 mTorr) for further purification, yielding 1.6 g (77%) of pure **4**. X-ray quality crystals were obtained by cooling a concentrated hexanes solution to –30 °C. ^{1}H NMR: (C_6D_6; δ) 12.3, 40.9 ppm. ^{1}H NMR: (C_4D_8O; δ) 11.0, 34.1 ppm. EA (found/calculated): C (48.62/48.22), H (10.64/10.48) %. $\mu_{eff} = 6.07$ B.M. $E_{pa} = –0.14$ V vs $[FeCp_2]^{0/+}$ in THF ($\nu = 200$ mVs^{-1}).

[(allyl^{TMS2})Mn{C(SiMe$_3$)$_3$}(quinuclidine)] (5): Compound **2** (0.23 g, 0.32 mmol) was dissolved in hexanes (15 mL) in a vial in the glovebox, quinuclidine (0.37 g, 0.33 mmol) was added at room temperature, and the reaction was stirred for 2 d. Solids were removed by centrifugation and the clear mother liquor was evaporated to dryness to give a sticky red solid. Sublimation at 90 °C (5 mTorr) gave a pure sample (0.20 g, 52%, note: higher sublimation temperatures should be avoided since complete decomposition was observed after 3 h at 110 °C). X-ray quality crystals were obtained from a concentrated pentane solution at –30 °C. ^{1}H NMR: (C_6D_6; δ) 5.6, 16.9, 49.1 ppm. EA (found/calculated): C (52.69/53.55), H (10.64/10.54), N (2.62/2.40) %. $\mu_{eff} = 5.91$ B.M. $E_{pa} = –0.14$ V vs $[FeCp_2]^{0/+}$ in THF ($\nu = 200$ mVs^{-1}).

[(allyl^{TMS2})Mn{C(SiMe$_3$)$_3$}(dmap)] (6): Compound **2** (0.53 g, 0.72 mmol) was dissolved in hexanes (10 mL) in a vial in the glovebox, a solution of dmap (0.89 g, 0.72 mmol) in toluene (5 mL) was added at room temperature, and the reaction was stirred overnight. Solids were removed by centrifugation and the clear mother liquor was evaporated to dryness. The residue was redissolved in hexanes and crystallized at –30 °C (0.30 g, 70%). X-ray quality crystals were obtained from a concentrated hexane solution at –30 °C. Compound **6** was found to sublime at 115 °C with substantial accompanying thermal decomposition, so sublimation was avoided as a method of purification. ^{1}H NMR: (C_6D_6; δ) 11.6, 19.9, 35.0 ppm. ^{1}H NMR: (C_4D_8O; δ) 9.7, 16.9, 28.0 ppm. EA (found/calculated): C (52.18/52.56), H (9.80/9.84), N (5.05/4.72) %. $\mu_{eff} = 5.63$ B.M. $E_{pa} = –0.27$ V vs $[FeCp_2]^{0/+}$ in THF ($\nu = 200$ mVs^{-1}).

[(allyl^{TMS2})Mn{C(SiMe$_3$)$_3$}] (7): BPh_3 (0.16 g, 6.57 mmol) was added to a sublimed sample of **4** (0.36 g, 6.57 mmol) in 10 mL of pentane. The reaction was stirred for 2 h, during which time white solids precipitated from solution. Solids were removed by centrifugation and identified as $Ph_3B(PMe_3)$ by

NMR spectroscopy [in C_6D_6, ^1H δ: 7.45 (d, 6H, $^1J_{HH} = 7.4$ Hz, Ph-*o*), 7.30 (app. t, 6H, $^1J_{HH} = 7.4$ Hz, Ph-*m*), 7.22 (t, 3H, $^1J_{HH} = 7.4$ Hz, Ph-*p*), 0.54 (d, 9H, $^1J_{H\text{-}P} = 9.8$ Hz, PMe_3) ppm; ^{31}P δ: –15.45 ppm; ^{11}B δ: –7.51 ppm]. The bright red supernatant was separated and evaporated to dryness to give a red oil which was sublimed at 50 °C (5 mTorr) using a dry ice cooled cold finger. The compound sublimed on the cold finger as a viscous oil, which was quickly taken into the glove box and removed by washing with pentane (0.28 g, 88%). After removal of pentane in vacuo and cooling to –25 °C in the glove box freezer, the oil solidified over a period of days to weeks (crystallization was immediate if a small amount of solid **7** was added to the oil to 'seed' the crystallization process). X-ray quality crystals were obtained from a highly concentrated pentane solution at –25 °C. PXRD could not be performed due to the waxy nature of the solids. A satisfactory elemental analysis was not obtained; we attribute this to the waxy nature of **7**, which resulted in smearing of a small amount of compound on the walls of the tin capsules, some of which was likely above the level at which the vials were sealed (this material would have decomposed upon removal from the glove box, resulting in low %C and %H values). ^1H NMR: (C_6D_6; δ) 22.4, 68.9 ppm. EA (found/calculated): C (46.70/48.35), H (10.05/10.25) %. $\mu_{eff} = 5.97$ B.M.

DFT Calculations: All structures were fully optimized with the ADF DFT package (SCM, version 2013.01).[43] Calculations were conducted using the zero-order regular approximation (ZORA)[44] for relativistic effects, and 1996 Perdew-Burke-Ernzerhof exchange and correlation for the GGA part of the density functional (PBE),[45] combined with Grimme's DFT-D3-BJ dispersion correction.[46] All calculations on manganese(II) complexes were unrestricted with 5 unpaired electrons. Preliminary geometry optimizations were conducted with frozen cores corresponding to the configuration of the preceding noble gas (core = medium) using a double-ζ basis set with one polarization function (DZP), an integration value of 5, and default convergence criteria. These structures were further refined using an all-electron TZ2P basis set (the size and quality of ADF basis sets increases in the order SZ < DZ < DZP < TZP < TZ2P < QZ4P), an integration value of 7, and a convergence gradient of 0.0001.

The structure of **7** in which the Mn–C(1) and Mn–C(3) distances are set to have a single freely refining value was calculated starting from the un-restrained structure of **7**. This was achieved by: (a) geometry re-optimization using the RESTRAINT keyword to set both Mn–C distances to 2.35 Å, followed by (b) geometry optimization of the resulting structure using internal coordinates with a single variable for both the Mn–C(1) and Mn–C(3) distances in the z-matrix; the starting value for this variable was defined as 2.35 Å using the GEOVAR keyword.

Analytical frequency calculations showed: (a) no imaginary frequencies in the cases of **4**, **7**, $\mathbf{7^{ss}}$, and [(*syn*,*anti*-allyl^{TMS2})Mn{C(SiH_3)$_3$}], consistent with converged minima, and (b) one imaginary frequency at –12 cm^{-1} in the case of [(*syn*,*anti*-allyl^{TMS2})MnMe]. This imaginary frequency is associated with a slight rotation of the trimethylsilyl groups of the allyl group, and not with changes involving the core of the molecule, so the structure of [(allyl^{TMS2})MnMe] can still be considered to have converged to a minumum. Analytical frequency calculations were also used to obtain free energy (G) values using the equation provided in the ADF manual [G = total bonding energy + total nuclear internal energy + pV – (T * total entropy) where T = 298 K and pV = nRT = 0.592 kcal mol^{-1}]. Visualization of the computational results was performed using the ADF-GUI (SCM) or Discovery Studio Visualizer (Accelrys).

ASSOCIATED CONTENT

Supporting Information. Modified syntheses for H[allyl^{TMS2}] and K[allyl^{TMS2}], Evans magnetic measurement details, the X-ray structure of **2**, ^{1}H NMR spectra of **2**-**7**, experimental and calculated PXRDs for **2**-**6**, and additional computational details. CCDC 952943-952948 contain the cif files for **2**-**7**, respectively.

AUTHOR INFORMATION

Corresponding Author

* Phone: 905-525-9140, Fax: 905-522-2509. E-mail: emslied@mcmaster.ca.

ACKNOWLEDGMENT

D.J.H.E. thanks Intel Corporation for funding through the Semiconductor Research Corporation (SRC) and NSERC of Canada for a Discovery grant. We are grateful to Dr. Patricio E. Romero of Intel Corporation for simultaneous TGA/DSC measurements on compound **4**.

REFERENCES

(1) Andersen, R. A.; Carmonaguzman, E.; Gibson, J. F.; Wilkinson, G. *J. Chem. Soc. Dalton Trans.* **1976**, 2204.

(2) a) Howard, C. G.; Wilkinson, G.; Thorntonpett, M.; Hursthouse, M. B. *J. Chem. Soc. Dalton Trans.* **1983**, 2025. b) Howard, C. G.; Girolami, G. S.; Wilkinson, G.; Thorntonpett, M.; Hursthouse, M. B. *J. Chem. Soc. Dalton Trans.* **1983**, 2631. c) Kennedy, A. R.; Klett, J.; Mulvey, R. E.; Robertson, S. D. *Eur. J. Inorg. Chem.* **2011**, 4675. d) Campora, J.; Palma, P.; Perez, C. M.; Rodriguez-Degado, A.; Alvarez, E.; Gutierrez-Puebla, E. *Organometallics* **2010**, *29*, 2960.

(3) a) Crewdson, P.; Gambarotta, S.; Yap, G. P. A.; Thompson, L. K. *Inorg. Chem.* **2003**, *42*, 8579. b) Alberola, A.; Blair, V. L.; Carrella, L. M.; Clegg, W.; Kennedy, A. R.; Klett, J.; Mulvey, R. E.; Newton, S.; Rentschler, E.; Russo, L. *Organometallics* **2009**, *28*, 2112. c) Morris, R. J.; Girolami, G. S. *Organometallics* **1989**, *8*, 1478. d) Blair, V. L.; Clegg, W.; Conway, B.; Hevia, E.; Kennedy, A.; Klett, J.; Mulvey, R. E.; Russo, L. *Chem. Eur. J.* **2008**, *14*, 65. e) Bart, S. C.; Hawrelak, E. J.; Schmisseur, A. K.; Lobkovsky, E.; Chirik, P. J. *Organometallics* **2004**, *23*, 237.

(4) a) Girolami, G. S.; Wilkinson, G.; Galas, A. M. R.; Thorntonpett, M.; Hursthouse, M. B. *J. Chem. Soc. Dalton Trans.* **1985**, 1339. b) Girolami, G. S.; Howard, C. G.; Wilkinson, G.; Dawes, H. M.; Thorntonpett, M.; Motevalli, M.; Hursthouse, M. B. *J. Chem. Soc. Dalton Trans.* **1985**, 921. c) Hitchcock, P. B.; Lappert, M. F.; Leung, W. P.; Buttrus, N. H. *J. Organomet. Chem.* **1990**, *394*, 57. d) Al-Juaid, S. S.; Eaborn, C.; El-Hamruni, S. M.; Hitchcock, P. B.; Smith, J. D.; Can, S. E. S. *J. Organomet. Chem.* **2002**, *649*, 121.

(5) Buttrus, N. H.; Eaborn, C.; Hitchcock, P. B.; Smith, J. D.; Sullivan, A. C. *Chem. Commun.* **1985**, 1380.

(6) Engerer, L. K.; Carlson, C. N.; Hanusa, T. P.; Brennessel, W. W.; Young, V. G. *Organometallics* **2012**, *31*, 6131.

(7) 18-electron carbonyl complexes: a) Brookhart, M.; Yoon, J.; Noh, S. K. *J. Am. Chem. Soc.* 1989, **111**, 4117; b) Perez, J.; Riera, L.; Riera, V.; Garcia-Granda, S.; Garcia-Rodriguez, E. *J. Am. Chem. Soc.* 2001, **123**, 7469; c) Perez, J.; Riera, L.; Riera, V.; Garcia-Granda, S.; Garcia-Rodriguez, E.; Miguel, D. *Organometallics* 2002, **21**, 1622; d) Morales, D.; Clemente, M. E. N.; Perez, J.; Riera, L.; Riera V.; Miguel, D. *Organometallics* 2003, **22**, 4124.

(8) 18-electron nitrosyl complexes; see for example: a) Ng, S. H. K.; Adams C. S.; Legzdins, P. *J. Am. Chem. Soc.* 2002, **124**, 9380; b) Tsang, J. Y. K.; Buschhaus, M. S. A.; Graham, P. M.; Semiao, C. J.; Semproni, S. P.; Kim S. J.; Legzdins, P. *J. Am. Chem. Soc.* 2008, **130**, 3652; c) Tran, T.; Chow, C.; Zimmerman, A. C.; Thibault, M. E.; McNeil W. S.; Legzdins, P. *Organometallics* 2011, **30**, 735.

(9) Copper(III) complexes detected at –100 °C: a) Bartholomew, E. R.; Bertz, S. H.; Cope, S.; Murphy M.; Ogle, C. A. *J. Am. Chem. Soc.* 2008, **130**, 11244; b) Bertz, S. H.; Hardin, R. A.; Murphy, M. D.; Ogle, C. A.; Richter J. D.;Thomas, A. A. *J. Am. Chem. Soc.* 2012, **134**, 9557.

(10) Square planar group 10 complexes; see for example: a) Hayashi, Y.; Nakamura Y.; Isobe, K. *J. Chem. Soc. Chem. Commun.* 1988, 403; b) Ogoshi, S.; Tonomori, K.; Oka M.; Kurosawa, H. *J. Am. Chem. Soc.* 2006, **128**, 7077; c) Chernyshova, E. S.; Goddard R.; Porschke, K. R. *Organometallics* 2007, **26**, 3236.

(11) Trivalent group 9 complexes (18 elec.): a) Nehl, H. *Chem. Ber.-Recl.* 1993, **126**, 1519; b) Bleeke, J. R.; Donnay E.; Rath, N. P. *Organometallics* 2002, **21**, 4099; c) McGhee W. D.; Bergman, R. G. *J. Am. Chem. Soc.* 1988, **110**, 4246.

(12) [Cp*Fe(η^3-allyl)Me] (presumed low-spin by analogy with $FeCp_2^+$): Furstner, A.; Martin, R.; Krause, H.; Seidel, G.; Goddard R.; Lehmann, C. W. *J. Am. Chem. Soc.* 2008, **130**, 8773.

(13) Tetravalent group 8 complexes (18 elec.): a) Nagashima, H.; Ara, K. I.; Yamaguchi K.; Itoh, K. *J. Organomet. Chem.* 1987, **319**, C11; b) Itoh K.; Fukahori, T. *J. Organomet. Chem.* 1988, **349**, 227; c) Mui, H. D.; Brumaghim, J. L.; Gross C. L.; Girolami, G. S. *Organometallics* 1999, **18**, 3264.

(14) Group 6 complexes (16 and 18 elec.): a) Benn, R.; Brock, T. H.; Dias, M.; Jolly, P. W.; Rufinska, A.; Schroth, G.; Seevogel K.; Wassmuth, B. *Polyhedron* 1990, **9**, 11; b) Benn, R.; Brock, T. H.; Jolly, P. W.; Rufinska A.; Schroth, G. *Polyhedron* 1990, **9**, 23.

(15) Dimetallic complexes (W and Os): a) Chisholm, M. H.; Folting, K.; Heppert J. A.; Streib, W. E. *J. Chem. Soc. Chem. Commun.* 1985, 1755; b) Tooze, R. P.; Wilkinson, G.; Motevalli M.; Hursthouse, M. B. *J. Chem. Soc. Dalton Trans.* 1986, 2711.

(16) Open-shell complexes of V and Mo: a) Hessen, B.; Lemmen, T. H.; Luttikhedde, H. J. G.; Teuben, J. H.; Petersen, J. L.; Huffman, J. C.; Jagner S.; Caulton, K. G. *Organometallics* 1987,

6, 2354; b) Barron, A. R.; Anderson, S. J.; McGregor K.; Wilkinson, G. *Polyhedron* 1989, **8**, 2599.

(17) Group 4 complexes: a) Erker, G.; Engel, K.; Dorf, U.; Atwood J. L.; Hunter, W. E. *Angew. Chem. Int. Ed. Engl.* 1982, **21**, 914; b) Tjaden, E. B.; Casty G. L.; Stryker, J. M. *J. Am. Chem. Soc.* 1993, **115**, 9814; c) Erker, G.; Berg, K.; Benn R.; Schroth, G. *Chem. Ber.-Recl.* 1985, **118**, 1383; d) Rodriguez G.; Bazan, G. C. *J. Am. Chem. Soc.* 1997, **119**, 343; e) Voth, P.; Fraser, C.; Graham, T.; Zhu, C. B.; Gauld J.; Stephan, D. W. *Organometallics* 2006, **25**, 4779.

(18) Maekawa, M.; Romelt, M.; Daniliuc, C. G.; Jones, P. G.; White, P. S.; Neese, F.; Walter, M. D. *Chem. Sci.* **2012**, *3*, 2972.

(19) Alvarez, C. S.; Boss, S. R.; Burley, J. C.; Humphry, S. M.; Layfield, R. A.; Kowenicki, R. A.; McPartlin, M.; Rawson, J. M.; Wheatley, A. E. H.; Wood, P. T.; Wright, D. S. *Dalton Trans.* **2004**, 3481.

(20) Layfield, R. A. *Chem. Soc. Rev.* **2008**, *37*, 1098.

(21) ALD of manganese metal is of particular interest in light of reports that copper-manganese alloys can be used for self-formation of a $MnSi_xO_y$ diffusion barrier at the interface between copper interconnect wiring and silicon- and oxygen-rich dielectric materials. Additionally, ultra-thin manganese metal, MnO_x and MnN_x layers deposited directly on a low-k dielectric such as SiCOH ('organosilicate glass') by Chemical Vapor Deposition (CVD) or Plasma-Enhanced CVD (PECVD) are reported to be highly effective copper diffusion barriers. These manganese-containing barrier layers have been proposed as replacements for more conventional Ta/TaN, Ti/TiN, W/TiN, Ru/TaN, or Mo/WN barrier layers in future microprocessors. See for example: a) Phuong, N. M.; Sutou, Y.; Koike, J. *J. Phys. Chem. C* **2013**, *117*, 160, and references therein; b) Kurokawa, A.; Sutou, Y.; Koike, J.; Hamada, T.; Matsumoto, K.; Nagai, H.; Maekawa, K.; Kanato, H. *Jpn. J. Appl. Phys.* **2013**, *52*, 05FA02; c) Iijima, J.; Fujii, Y.; Neishi, K.; Koike, J. *J. Vac. Sci. Technol., B* **2009**, *27*, 1963; d) Jourdan, N.; Barbarin, Y.; Croes, K.; Siew, Y. K.; Van Elshocht, S.; Tokei, Z.; Vancoille, E. *ECS Solid State Lett.* **2013**, *2*, P25; e) Au, Y.; Lin, Y. B.; Gordon, R. G. *J. Electrochem. Soc.* **2011**, *158*, D248; f) Kalutarage, L. C.; Martin, P. D.; Heeg, M. J.; Winter, C. H. *J. Am. Chem. Soc.* **2013**, *135*, 12588; g) Knisley, T. J.; Saly, M. J.; Heeg, M. J.; Roberts, J. L.; Winter, C. H. *Organometallics* **2011**, *30*, 5010.

(22) Eaborn, C.; Hitchcock, P. B.; Smith, J. D.; Sullivan, A. C. *J. Chem. Soc. Chem. Commun.* **1985**, 534.

(23) Simpson, C. K.; White, R. E.; Carlson, C. N.; Wrobleski, D. A.; Kuehl, C. J.; Croce, T. A.; Steele, I. M.; Scott, B. L.; Young, V. G.; Hanusa, T. P.; Sattelberger, A. P.; John, K. D. *Organometallics* **2005**, *24*, 3685.

(24) Solomon, S. A.; Layfield, R. A. *Dalton Trans.* **2010**, *39*, 2469. Chmely, S. C.; Hanusa, T. P. *Eur. J. Inorg. Chem.* **2010**, 1321.

(25) a) Although **2** was pure by elemental analysis, the crystal used for X-ray diffraction contained a 89:11 mixture of chloride and bromide, presumably due to a small amount of bromide in the commercial $MnCl_2$ starting material. b) One of the two molecules in the unit cell of **3** is disordered over two positions; metrical parameters are discussed only for the disorder-free molecule.

(26) a) Evans, D. F. *J. Chem. Soc.* **1959**, 2003. b) Schubert, E. M. *J. Chem. Educ.* **1992**, *69*, 62.

(27) Cordero, B.; Gómez, V.; Platero-Prats, A. E.; Revés, M.; Echeverría, J.; Cremades, E.; Barragán, F.; Alvarez, S. *Dalton Trans.* **2008**, 2832.

(28) In all X-ray and calculated structures, C(1) is the terminal carbon atom of the allyl unit in closest proximity to Mn.

(29) The residual mass of 2 % in the TGA at 0.5 Torr may be due to small amounts of chemical decomposition as a result of the extreme moisture and oxygen-sensitivity of the compounds and the small masses involved in the TGA measurements.

(30) Layfield, R. A.; Humphrey, S. M. *Angew. Chem. Int. Ed.* **2004**, *43*, 3067.

(31) Ligand redistribution from **7** to form previously reported $[Mn\{C(SiMe_3)_3\}_2]$ and unknown $[Mn(allyl^{TMS2})_2]$ was excluded by comparison of the ^1H NMR spectrum of **7** with that of an independently synthesized sample of $[Mn\{C(SiMe_3)_3\}_2]$ in C_6D_6: reference 13.

(32) a) Bartholomew, E. R.; Bertz, S. H.; Cope, S.; Murphy, M.; Ogle, C. A. *J. Am. Chem. Soc.* **2008**, *130*, 11244. b) Bertz, S. H.; Hardin, R. A.; Murphy, M. D.; Ogle, C. A.; Richter, J. D.; Thomas, A. A. *J. Am. Chem. Soc.* **2012**, *134*, 9557.

(33) a) Benn, R.; Brock, T. H.; Dias, M.; Jolly, P. W.; Rufinska, A.; Schroth, G.; Seevogel, K.; Wassmuth, B. *Polyhedron* **1990**, *9*, 11. b) Benn, R.; Brock, T. H.; Jolly, P. W.; Rufinska, A.; Schroth, G. *Polyhedron* **1990**, *9*, 23.

(34) Chisholm, M. H.; Folting, K.; Heppert, J. A.; Streib, W. E. *J. Chem. Soc. Chem. Commun.* **1985**, 1755.

(35) Calculated structures for $[Mn(\eta^3\text{-}C_3H_3R_2)(\eta^1\text{-}C_3H_3R_2)_2]^-$ (R = H or $SiMe_3$) also featured a significantly asymmetric bonding mode for the η^3-coordinated allyl ligand: R. A. Layfield, M. Buhl and J. M. Rawson, *Organometallics*, 2006, **25**, 3570.

(36) A value of 2.90 Å was used for Mn–C(2) since the corresponding bond lengths for the η^1-allyl^{TMS2} ligands in $[Li(THF)_4][Mn(allyl^{TMS2})_3]$, $K_2[Mn(allyl^{TMS2})_4]$, $[Mn(allyl^{TMS2})_2(THF)_2]$ and $[Mn(allyl^{TMS2})_2(\kappa^2\text{-tmeda})]$ are between 2.88 and 2.99 Å: references 15 and 16.

(37) a) Ni, C. B.; Fettinger, J. C.; Long, G. J.; Power, P. P. *Dalton Trans.* **2010**, *39*, 10664. b) Ni, C. B.; Power, P. P. *Organometallics* **2009**, *28*, 6541. c) Sattler, A.; Parkin, G. *J. Am. Chem. Soc.* **2012**, *134*, 2355.

(38) LeSuer, R. J.; Buttolph, C.; Geiger, W. E. *Anal. Chem.* **2004**, *76*, 6395.

(39) Uhl, W.; Jantschak, A.; Saak, W.; Kaupp, M.; Wartchow, R. *Organometallics* **1998**, *17*, 5009.

(40) Avent, A. G.; Eaborn, C.; Hitchcock, P. B.; Lawless, G. A.; Lickiss, P. D.; Mallien, M.; Smith, J. D.; Webb, A. D.; Wrackmeyer, B. *J. Chem. Soc. Dalton Trans.* **1993**, 3259.

(41) Eaborn, C.; Hitchcock, P. B.; Smith, J. D.; Sullivan, A. C. *J. Chem. Soc. Chem. Commun.* **1983**, 827.

(42) Fraenkel, G.; Chow, A.; Winchester, W. R. *J. Am. Chem. Soc.* **1990**, *112*, 1382.

(43) a) ADF2010, SCM, Theoretical Chemistry, Vrije Universiteit, Amsterdam, The Netherlands, http://www.scm.com. b) te Velde, G.; Bickelhaupt, F. M.; van Gisbergen, S. J. A.; Fonseca Guerra, C.; Baerends, E. J.; Snijders J. G.; Ziegler, T. *J. Comput. Chem.* **2001**, *22*, 931. c) Fonseca Guerra, C.; Snijders, J. G.; te Velde G.; Baerends, E. J. *Theor. Chem. Acc.* **1998**, *99*, 391.

(44) a) van Lenthe, E.; Baerends, E. J.; Snijders, J. G. *J. Chem. Phys.* **1993**, *99*, 4597. b) van Lenthe, E.; Baerends, E. J.; Snijders, J. G. *J. Chem. Phys.* **1994**, *101*, 9783. c) van Lenthe, E.; Ehlers, A.; Baerends, E.-J. *J. Chem. Phys.* **1999**, *110*, 8943. d) van Lenthe, E.; Snijders, J. G.; Baerends, E. J. *J. Chem. Phys.* **1996**, *105*, 6505. e) van Lenthe, E.; van Leeuwen, R.; Baerends, E. J.; Snijders, J. G. *Int. J. Quantum Chem.* **1996**, *57*, 281.

(45) Perdew, J. P.; Burke, K.; Ernzerhof, M. *Phys. Rev. Lett.* **1996**, *77*, 3865.

(46) a) Grimme, S.; Ehrlich, S.; Goerigk, L. *J. Comput. Chem.* **2011**, *32*, 1457. b) Grimme, S.; Anthony, J.; Ehrlich, S.; Krieg, H. *J. Chem. Phys.* **2010**, *132*, 154104.

For Table of Contents Use Only

Manganese(II) Alkyl / π-Allyl Complexes Resistant to Ligand Redistribution

Preeti Chadha,[a] David J. H. Emslie[a,]* and Hilary A. Jenkins[b]

TOC Text: A family of mixed alkyl / π-allyl manganese(II) complexes has been prepared, including [(allyl$^{\mathrm{TMS2}}$)Mn{C(SiMe$_3$)$_3$}(PMe$_3$)] and base-free [(allyl$^{\mathrm{TMS2}}$)Mn{C(SiMe$_3$)$_3$}]. These are the first high-spin d^5 mixed alkyl / allyl complexes, and [(allyl$^{\mathrm{TMS2}}$)Mn{C(SiMe$_3$)$_3$}] is the first thermally stable example of a mononuclear transition metal complex bearing only alkyl and allyl ligands.

TOC Graphic: